Hindawi Publishing Corporation
International Journal of Antennas and Propagation
Volume 2015, Article ID 270949, 10 pages
http://dx.doi.org/10.1155/2015/270949

Research Article

Propagation Measurement on Earth-Sky Signal Effects for High Speed Train Satellite Channel in Tropical Region at Ku-Band

Abdulmajeed H. J. Al-Jumaily,[1] A. Sali,[1] J. S. Mandeep,[2] and Alyani Ismail[1]

[1]*Department of Computer and Communication Systems Engineering, Universiti Putra Malaysia (UPM), 43400 Serdang, Selangor, Malaysia*
[2]*Department of Electrical, Electronic and Systems Engineering, Universiti Kebangsaan Malaysia (UKM), 43600 Bangi, Selangor, Malaysia*

Correspondence should be addressed to Abdulmajeed H. J. Al-Jumaily; abdulmajeedjasim@yahoo.com

Received 5 December 2014; Revised 14 February 2015; Accepted 24 February 2015

Academic Editor: Felipe Cátedra

Recent advances in satellite communication technologies in the tropical regions have led to significant increase in the demand for services and applications that require high channel quality for mobile satellite terminals. Determination and quantification of these requirements are important to optimize service quality, particularly in the Malaysian region. Moreover, the tests on current satellite propagation models were carried out at temperate regions whose environmental characteristics are much different from those in Malaysia. This difference renders these propagation models inapplicable and irrelevant to tropical regions in general. This paper presents the link characteristics observations and performance analysis with propagation measurements done in tropical region to provide an accurate database regarding rain and power arches supply (PAs) attenuations in the tropics for mobile scenarios. Hence, an extension for improving the performance assessment and analysis of satellite/transmission has been achieved. The Malaysia propagation measurement for mobile scenario (Malaysia-PMMS) enables first-hand coarse estimation and attenuation analysis, because the attenuation resulting from rain and PAs becomes easily amenable for measurement. Parallel to that, the measured attenuation has been compared with that of the simulated output at noise floor level. The underlying analytical tool is validated by measurements specific at tropical region, for dynamic model of mobile satellite links operating at higher than 10 GHz.

1. Introduction

There are many satellites orbiting the earth, which help us in communications. The role of satellite communications in our day-to-day life keeps on increasing [1]. The television we watch and the internet we browse are controlled by satellite technology [2]. The microwave signals used in satellite communication are of high frequency. The increasing demand of satellite technology that utilizes high frequency microwaves has increased the need for wide bands [3]. Operation of high frequency bands, such as the Ku-band, for satellite communications has many advantages. First, it relieves congestion in the lower frequencies shared with terrestrial links. Second, it exploits larger bandwidths available at higher frequencies. Third, it enables cheaper implementation of spectrum conservation techniques with more efficient use of the geostationary curve [4, 5]. Instead of L, S, or C bands, researches of the last decades have considered large bandwidth at Ku and Ka band for spectrum congestion. High frequency bands (e.g., Ku-band), like broadband fixed satellite services, are seldom used, especially in public transport vehicles, such as high velocity trains and tramways. Owing to troposphere-based impairment, the propagation channel of mobile application is strongly affected by shadowing or scattering.

Ku-band is used extensively in maritime applications and is also used in a number of railroads. Environmental factors like shadowing and scattering are affecting powerfully the propagation channel in the mobile cases. Deep knowledge in dynamic properties of channel is needed. Design of fade mitigation techniques to overcome this problem requires in-depth knowledge of the channel mobility properties to be achieved through development of channel models. Most of

recent researches conducted in high speed train scenario had been attentive to the lower frequency L, S, and C bands. Satellite propagation models for mobile scenarios at equatorial regions are urgently needed, because there has so far been no reliable and accurate method for assessment of the mobile scenarios with regard to attenuation from rain and PAs, which is characteristic of tropical regions, particularly Malaysia. Moreover, the current satellite propagation models are meant only for temperate regions whose environmental characteristics are totally different from those of Malaysia. Because of this difference, the existing propagation measurement is inaccurate and irrelevant to the tropical regions in general and Malaysia in particular. To address the current issues relating to propagation impairment in Malaysia, devising an appropriate propagation model for mobile scenarios is required which in turn can ensure reliable assessment of the attenuation output from rain and power arch supply (PAs).

The following are the four major causes of signal degradation: diffraction of (PAs), depending on the geometry of the satellite link; deep fading (trees along railroad or high-rise buildings), multipath effect caused primarily by hails or nearby buildings [6]; Doppler effect, which depends on rain attenuation and the speed and direction of train movement; and antenna tracking error. The satellite communication system designers will have to keep in mind these four major causes in setting out to build a well-formulated model to predict the quality of services (QoS). Several solutions are proposed to ensure digital TV reception on board high speed trains in Europe, using a Ku-band satellite link [7]. Additionally, [8] takes additional comprehensive view of the railway satellite channel RSC by introducing a different stochastic dynamic model of rain fading in mobile satellite systems on top of the diffraction because of PAs. On the other hand, [9] deals with the analysis of advanced fade countermeasures for supporting DVB-S2 reception by mobile terminals mounted on high speed trains. Moreover, the current satellite propagation models are done at temperate regions which exhibit different environmental characteristics seen in Malaysia. This makes their propagation model inaccurate and irrelevant to the tropical regions in general and Malaysia in particular.

In this paper, the proposed Malaysia propagation measurement setup for mobile scenario (Malaysia-PMMS) enables first-hand coarse estimation of attenuation, due to its simplicity. The attenuations resulting from rain and PAs were measured independently. The obtained output was statistically analyzed to calculate the total attenuation composite PAs with rain time series synthesizer. The attenuation measured from power arch supply was conducted to the simulated output at noise floor level. This comparison is useful to validate attenuation of PAs.

The remainder of the paper is organized as follows: Section 2 presents the methodology, Section 3 the experimental setup for mobility impairments, and Section 4 the results and discussion. Finally, Section 5 presents the conclusions.

2. Methodology

According to Friis transmission equation, the frequency is directly proportional to the signal power attenuation and, hence, to the carrier-to-noise ratio, which could also lead to the increase in the error rates. For lower frequencies, below 3 GHz, the ionospheric scintillation significantly affects the signal quality. This effect starts to disappear as the frequency increases above that value [10]. Moreover, raindrops in the link between the satellite and Earth station exert a paramount effect on the quality of the signal at higher frequencies, particularly above 10 GHz [11]. To extract and analyze the atmospheric losses as well as the mobility effects out of the other impairments, several experiments were conducted, which considered a mobile scenario. Two scenarios were considered in this work, which are (i) train moving at different speeds up to 150 km/hr and (ii) train moving at a constant speed (150 km/h) under link obstacles, namely, high trees and buildings, bridges, and tunnels (Figure 1).

2.1. The Effects on High Speed Train Satellite Channel in Remote Areas. Depending on the railway path chosen, the layout and geometry of the obstacles can significantly change. From previous works, it is known that attenuation introduced by these kinds of obstacles can be accurately modeled using knife-edge diffraction theory [12]. For obstacles of two finite dimensions (e.g., tunnel, bridge, hills, or high-rise building), the knife-edge attenuation was computed as the ratio between the fields received in the presence and absence of the obstacles. The obstacles that our scenario faced are explained in Figures 2(a), 2(b), 2(c), and 2(d).

The obstacle had two finite dimensions, and the received field was hence the sum of the contributions coming from both sides of the obstacle. Therefore, the resulting attenuation was calculated using [12]

$$A_s = \left|\frac{E_1}{E_2}\right| = \frac{1}{\sqrt{2}}\left|\int_{V_0}^{\infty} e^{-j(\pi/2)V^2}\right| \quad V_0 = h\sqrt{\frac{2}{\lambda}\frac{a+b}{a\cdot b}}, \tag{1}$$

where a is the distance between obstacle and antenna, b is the distance between satellite and obstacle, λ is the wavelength, and h is the obstacle height above line of sight (LOS). For the scenario under discussion, (1) was modified with additional terms as shown in

$$\begin{aligned} A_{s(h)} &= \left|\frac{E_1}{E_0}\right| + \left|\frac{E_2}{E_0}\right| \\ &= \frac{1}{\sqrt{2}}\left(\left|\int_{V_0}^{\infty} e^{-j(\pi/2)V^2}dV\right|\right. \\ &\qquad \left. + \left|\int_{-\infty}^{V_0=h\sqrt{(2/\lambda)((a+b)/(a\cdot b))}} e^{-j(\pi/2)V^2}dV\right|\right), \end{aligned} \tag{2}$$

where d represents the width of the (PAs). Finally, using a directive antenna has been considered. This implies an increase in attenuation, because two diffracted rays reached the receiving antenna at different angles. The antenna detected the gain which depended on the variable. Anyway,

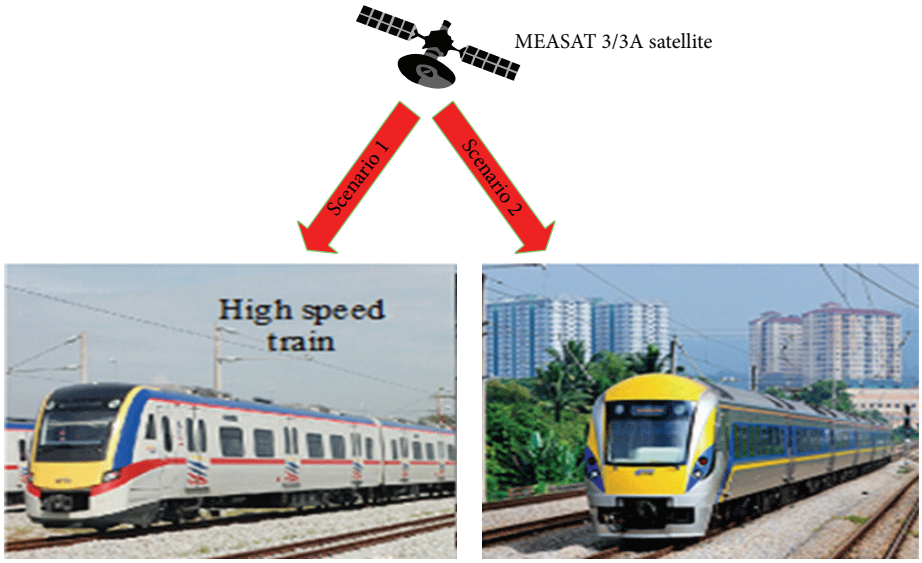

(a) Train moves at different speed (b) Train at constant speed

Figure 1: The scenarios for high speed train environment.

(a) PAs at the ETS station (b) Railroad

(c) PAs nearing the ETS station (d) Main ETS station at KL

Figure 2: Obstacles in Malaysia high speed train scenario.

Table 1: Parameters used for the two scenarios in temperate and tropical regions.

Parameters	Description	Our setup	Italy [12]
f	Frequency (GHz)	11.096	12
D	Diameter of antenna (m)	0.44	0.40
a	Distance between obstacle and antenna (m)	2	2.5
b	Distance between satellite and antenna (km)	36,000	36,000
d	Diameter of power arch (m)	0.60	0.40
Km/h	Train speed	150	300
Type	Signal	Modulated	CW beacon

it is lower than the achievable maximum. This resulted in a total attenuation of the following equations:

$$A_s = \frac{G(\alpha_1(h))}{G_{\max}} \left| \frac{E_1}{E_0}(h) \right| + \frac{G(\alpha_2(h))}{G_{\max}} \left| \frac{E_1}{E_0}(h) \right|, \quad (3)$$

$$G(\alpha) = \frac{\pi^2 \cdot D^2}{\lambda^2} \cdot \left(\frac{2 \cdot J_1(u)}{u} \right)^2, \quad (4)$$

$$u = \frac{\pi \cdot D}{\lambda} \sin(\alpha), \quad (5)$$

where $G_{\max} = (\pi^2 \cdot D^2/\lambda^2)$, $u = \pi \cdot D/\lambda \sin(\alpha)$, and $J_1(u)$ is the first order Bessel function of the first kind and it is a measuring for the antenna diameter. Formula (4) is valid for a generic circular aperture antenna. The corresponding space varying attenuation was computed using (1) to (4), with values extracted from a typical layout of the Italian railway for (a, b) and (d) [12]. Table 1 shows the parameters included in the models of both temperate and tropical regions. Thus, a further approval has been done.

2.2. Time Series for High Speed Train Satellite Channel at Ku-Band. Considering the two main impairments of the nearly LOS of mobile scenario because of attenuation due to power arches supply (PAs) and rain, (6) play an important role in developing the composite synthesizer of time series of mobile scenario at Ku-band and above [13]. Figure 4 shows the diagram of the total time series synthesizer. For the attenuation model, as a whole, rain attenuation measurement was executed before adding both attenuation factors. The PAs signal generator $P(t)$ produces pulses which contain unit amplitude when attenuation A_s is greater than 0 dB.

For example, let the intermission be $[0, h_0]$. If P_0 is the distance between subsequent PAs, the same attenuation will be repeated every P_0/V_t seconds, with k indicating the index of PAs. A potential understanding of the pulse series generator might be as follows:

$$\sum_k P\left(t - k\frac{P_0}{V_t}\right) = \sum_k \left[U\left(t - \frac{(k-1)P_0 - h_0}{V_t}\right) - U\left(t - \frac{(k-1)P_0}{V_t}\right) \right]. \quad (6)$$

A distance of $P_0 = 53$ m between every two (PAs) is used to compute the results in a duty cycle of 0.6%, considering $U(t)$ as the unit amplitude step function. The output of the total attenuation composite time series synthesizer given input parameters for a train speed of $V_t = 150$ km/h, regardless of total attenuation. The contribution of every attenuation factor is illustrated in Figure 20. The total attenuation depended on formula (6) [8].

Figure 5 shows the diagram of noise floor level. The noise floor is the measure of the signal created from the sum of all the noise sources and unwanted signals within a measurement system.

2.3. Doppler Effect Investigation. As the wave source and receiver move relative to each other, the frequency of the waves arriving at the receiver correspondingly changes. This phenomenon is known as the Doppler effect. The occurrence of Doppler shift makes the wireless channel fast-time variant and frequency selective as well as potential synchronization, channel estimation, and data recovery. The connection between the Doppler frequency shift (f_d) and the sender transmitted data on carrier frequency (f_c) is given by [14]

$$f_d = \left(\frac{V \cdot f_c}{c} \right) \cos\theta, \quad (7)$$

where (V) is the speed in m/s of the mobile traveling in straight line, (c) speed of light (3×10^8 m/s), and (θ) the angle of signal transmission between the transmitter and the receiver. The Doppler effect is one of the most significant phenomena, because it deserves attention whenever one has to deal with multicarrier access communication systems where a small amount of frequency variation can cause significant degradation in overall performance (Figure 6).

3. Experimental Setup for Mobility Impairments

To identify the error rates for the mobile scenario, we conducted several experiments considering the cases of quality degradation of signals received by a receiver mounted on a high speed train at different speeds from Kuala Lumpur to Ipoh, in Malaysia (Figure 7). These cases are listed as follows.

Scenario 1. The train moved at different speeds up to 150 km/hr. The received signal at zero speed (fixed) was also measured using the same mobile antenna system.

(a) ETS route map

(b) ETS under different types of obstacles: high-rise buildings and bridges

(c) ETS under different types of obstacles: tunnels, huge stations, and trees

Figure 3: Different types of obstacles: trees, buildings, bridges, and tunnels.

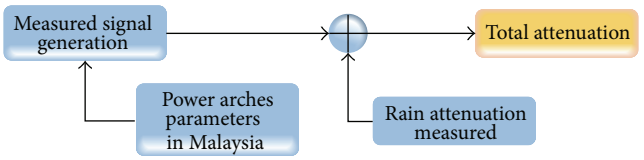

Figure 4: Block diagram of composite (PAs + rain) time series synthesizer.

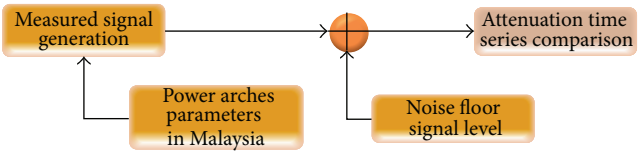

Figure 5: Block diagram measured with noise floor level.

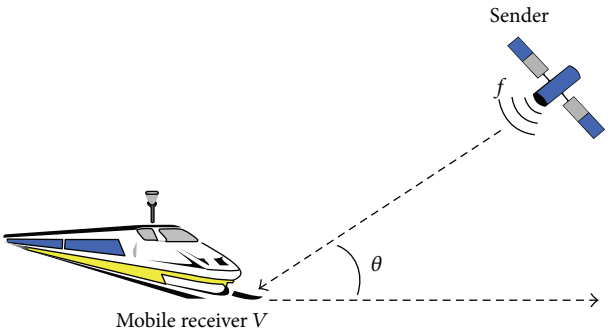

Figure 6: Doppler effect concept for mobile scenario.

Figure 7: High speed terminal, electrified train system (ETS).

Scenario 2. The train moved at a constant speed (150 km/h) under link obstacles, namely, high trees and buildings (approximately 11 and 30 m in height and 5 m away from the train, in average) alongside the train-track, tunnels, and bridges.

For the measurement setup, we used a 44 cm mobile antenna system mounted on the roof of a train. The mobile antenna system, pointing toward MEASAT 3/3A 91.5°E, had a high tracking speed (75°/sec) to reduce the tracking error as much as possible. The antenna system performed several principal functions, namely, detection, filtering, amplification, and downconversion to L-band 1.35 GHz, intermediate frequency (IF) using a 9.75 GHz local oscillator. The measurement setup is shown in Figure 8.

Once the signals were received by the mobile antenna system, they were immediately transmitted through the four

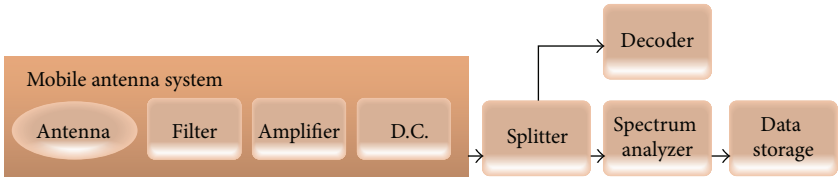

Figure 8: Measurement setup for the mobile terminals scenario.

Table 2: Satellite, antenna, and site specifications for mobile terminals.

Satellite, antenna, and specifications	Train
Satellite	MEASAT 3/3A
Satellite position	91.5°E
Frequency downlink (GHz)	11.096
Elevation angle of antenna (deg.)	76.5°
Diameter and height of antenna (m)	0.44 × 0.077
Weight (kg)	3.3
Tracking rate (deg.)	75°/sec
Polarization	Vertical

aforementioned processes and then split into two directions, one pointing to the decoder and the other to the spectrum analyzer, for data recognition and analysis. Table 2 shows the parameters satellite, antenna, and site parameters used for our measurement setup.

4. Results and Discussion

As mentioned earlier, the train gets close to the power arch's area; the obstacle enters the first Fresnel zone, which is about 2 m away from receiver antenna, where its width is around 44 cm and no free space conditions can be assumed. To signal attenuation, knife-edge diffraction models were considered. The knife-edge diffraction is represented by the ratio between the received field in the presence of obstacle and that in the free space. The attenuation of power arches supply is dependent on the height (h), which was around 1.6 m. The simulated event results for a mobile satellite antenna with a diameter of 44 cm are presented in Figure 9.

From the plots, it can be seen that the values were varied with changes in elevation angle and orientation of the mobile scenario. It can also be seen that the attenuation indicating the PAs is relevant to the value of 2 m on the average. Then, a distance of around 53 m between two subsequent PAs and a train speed of 150 km/h were considered. The fading event occurred, in the worst case, every 41.666 ms. The fluctuations around the free space loss condition (0 dB attenuation) are attributable to the train passes under the PAs. This intersects with Fresnel zones of different orders. These may be either in phase transmission causing constructive interference or out of phase causing destructive interference.

Figure 9 shows that the attenuation gain was approximately 44 dB, with $d = 60$ cm, $a = 2$ m, and $D = 44$ cm, and the downlink frequency is at 11.096 GHz based on the parameters used in Malaysia as tropical regions which

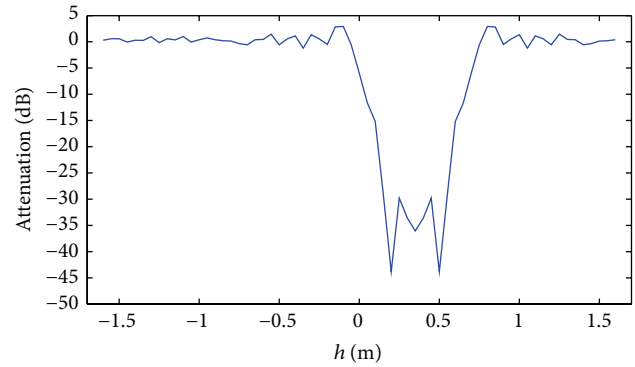

Figure 9: Attenuation owing to power arch supply (PAs) diffraction at Ku-band; the antenna diameter effect, line of sight (LOS) Malaysia parameters.

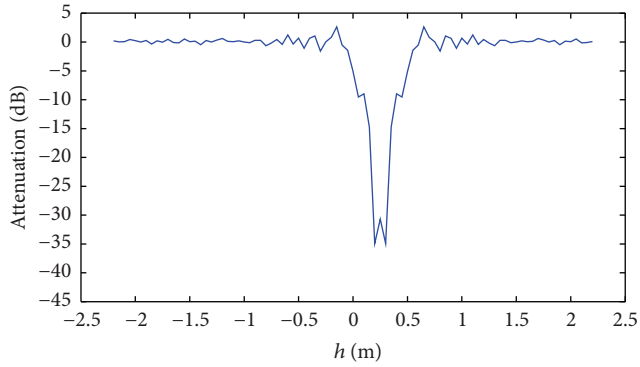

Figure 10: Attenuation owing to power arch supply (PAs) diffraction at Ku-band; the antenna diameter effect, line of sight (LOS) Italy parameters [12].

are different from those used in Italy as temperate regions. Therefore, depending on the specification used by the region or countries, the above mentioned parameters play a vital role in increasing the attenuation. For example, the distance between the antennas fixed on train roof and to the power arch supply, the diameter of antenna, and the width of power arch supply directly affect the attenuation and signal transmission.

Figure 10 shows that the simulated event attenuation loss was approximately 34 dB, with $d = 40$ cm, $a = 2.5$ m, and $D = 40$ cm and downlink frequency of 12 GHz at Ku-band depending on the parameters used in [12] Italy as temperate regions. As mentioned earlier, the parameters of the PAs, such as distance of antenna and width of PAs, along with the link

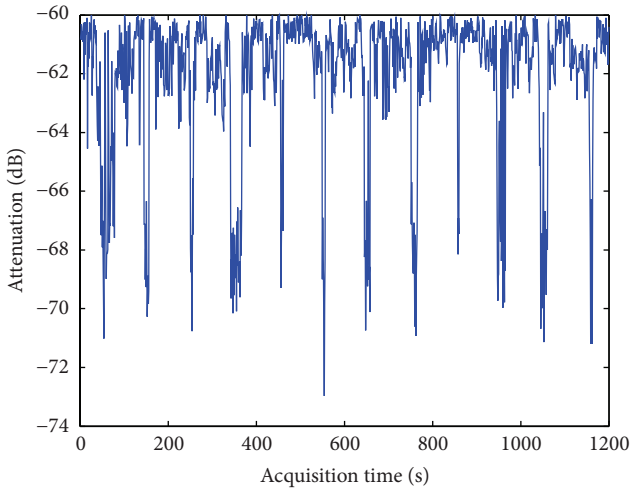

Figure 11: Measured attenuation of power arch supply.

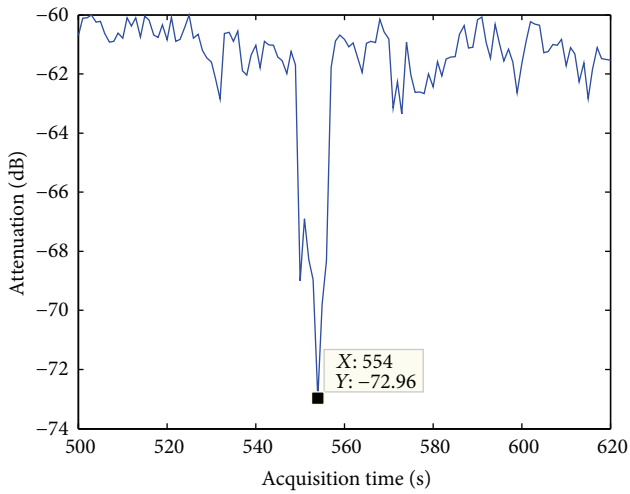

Figure 12: Measured attenuation of power arch supply.

parameters including both elevation angle and transmitted frequency, significantly affected the satellite communication link. That effect influences the performance metrics, such as attenuation.

Figures 11 and 12 show the attenuation of PAs, measured during the 1 hour starting from 7:00 pm to 8:00 pm on December 18, 2013. The sweeping was 1 second and the average data was recorded every 3 seconds. The impact was recorded as different attenuations during this time, because degradation happened before or after reaching the PAs (Figure 11). The attenuation was at its maximum when the train speed exceeded 150 km/h (554 seconds, 7:28 pm; 12.56 dB).

Figure 13 shows the measured rain attenuation loss in the received signal power. Time series was measured during the 1 hour in high speed train with speed 150 km/h, starting from 6:56 pm to 6:57 pm on December 18, 2013. Effective rain started at second number 1076, 5:56 pm, and reached the heavy rain level after 4 min, with maximum attenuation of

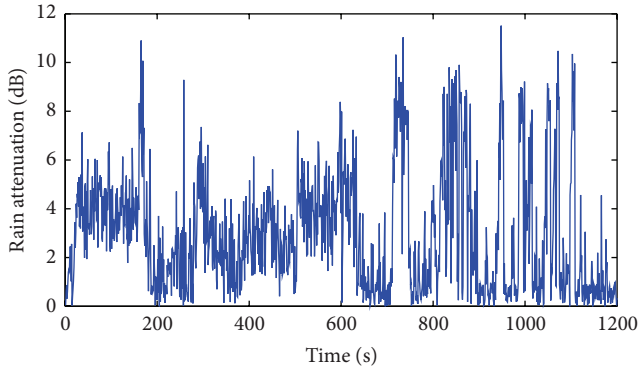

Figure 13: Measured rain attenuation when the train is in service.

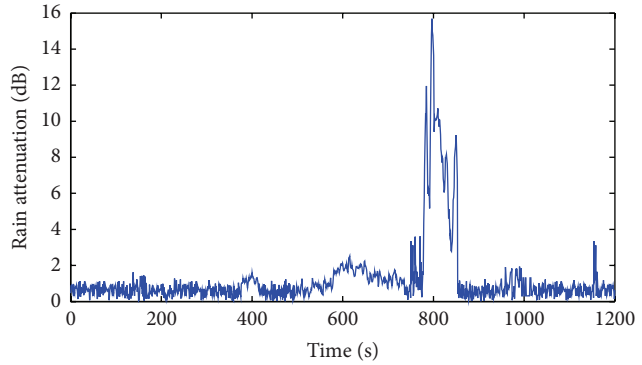

Figure 14: Measured rain attenuation stationary case.

nearly 11.512 dB. The rainfall rate started to decrease at second number 1124, 6:42 pm, to the other rainfall rate levels until second number 1147, 6:57 pm, when the rain stopped. The duration from 5:56 pm to 6:57 pm on December 18, 2013, was the time to read attenuations under the rainfalls while the duration from 7:00 pm to 8:00 pm of the same day was to read attenuations resulting from PAs as there were rain events during this duration. Thus, the rain attenuation measurements are obtained and separated from other attenuation measurements.

Figure 14 shows the measured rain attenuation loss in the received signal power when the train was stationary. Time series was measured during the 1 hour with stationary link, starting from 12:37 pm to 1:40 pm on December 24, 2013. Effective rain started at second number 779, 12:37 pm, and reached the heavy rain level after 5 min, with maximum attenuation of nearly 15.7 dB. The rainfall rate started to decrease at second number 883, 1:21 pm, to the other rainfall rate levels until second number 1158, 6:37 pm, when the rain stopped.

In the mobile scenario, to obtain a reliable performance evaluation of the signal detected by the mobile receiver attached to a train, several issues will have to be considered, which are already explained in Section 2. Movement of the communication link destination with respect to the source causes additional degradation to the signal quality level. The scenario consists of 11 stop-stations between KL and

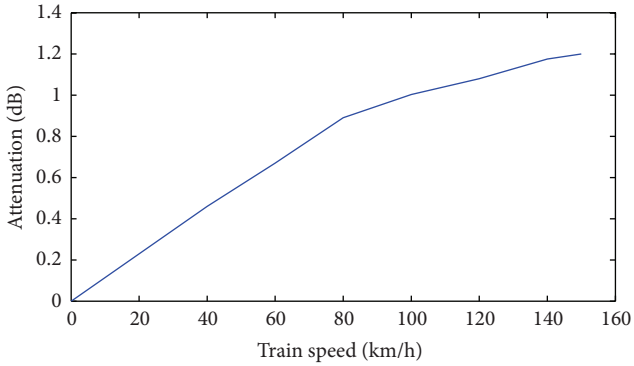

Figure 15: Attenuation measurement under different train speeds.

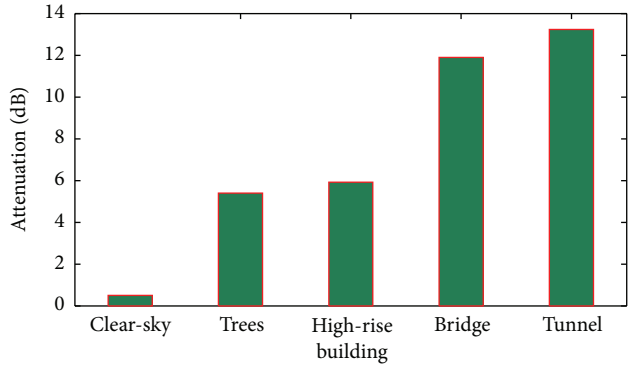

Figure 17: Attenuation due to different link obstacles with speed of 150 km/hr.

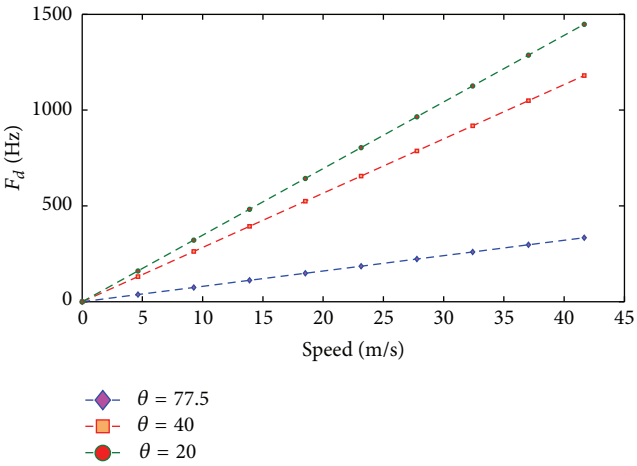

Figure 16: Worst case Doppler effect for mobile scenario.

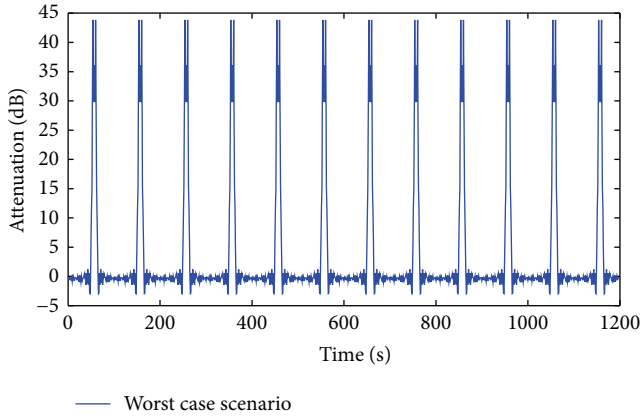

Figure 18: Worst case scenario within reason (PAs).

Ipoh, which leads to train speed between 0 and 150 km/h (referring to Figure 3). Figure 15 shows that attenuation increased slightly when the train speed increased; it increased by approximately 0.7 dB when the train moved at a speed of 60 km/hr. When the speed reached 80 km/hr, the attenuation slope changed, and with further increase in speed, the attenuation tended to attain slightly higher levels than that seen at speed 80 km/hr. Hence, the loss reached approximately 1.1 dB at 100 km/hr, 1.18 dB at 140 km/hr, and 1.20 dB at 150 km/hr.

In addition, the worst case Doppler shift simulation calculated (Figure 16) was considered assuming a train speed of up to $V_{\max} = 41.67$ m/s and using frequency measurements of signals sent out directly from the receiver. From Figure 16, it can be seen that the Doppler frequency (f_d) is in preoperational relationship with the carrier frequency (f_c). Using different elevation angles with high speed of train, 41.67 m/s, the highest F_d (Hz) was measured at angle 20° while the lowest was at 77.5°.

We made several experiments with the train moving at 150 km/hr in Kuala Lumpur under high trees and buildings (approximately 11 m and 30 m average height) along both sides of the rail track (referring to Figure 3). And the results are shown in Figure 17. The results show that these trees caused an additional average attenuation of 5.4 dB as compared with that under high-rise buildings, which is approximately 6 dB average attenuation compared with that under the clear-sky case. And, where the train passed underneath bridges at a speed of 150 km/hr, the attenuation was approximately 12 dB. When the train passed through a tunnel at the same speed, the attenuation reached approximately 13 dB indicating a significant loss in communication compared with that seen under the clear-sky mobile scenario. It would not exceed 13 dB, which is attributable to limitations in spectrum analyzer.

The propagation model can be applied to such an extracted worst case scenario. The example of attenuation time series should consider the effects of environment. To model mobile scenario environment, statistical features from a worst case scenario were extracted from simulated PAs. The simulation of worst case mobile scenario environment is illustrated in Figure 18, where the loss was approximately 44 dB.

Figure 19 shows different comparisons of the data collected in terms of attenuation of experimental time series. To get time series of similar behavior, data was inverted from the original time series. The data, plotted at noise floor level, shows an attenuation of 13 dB below the signal level at clear sky. The noise floor level refers to measurements of attenuation.

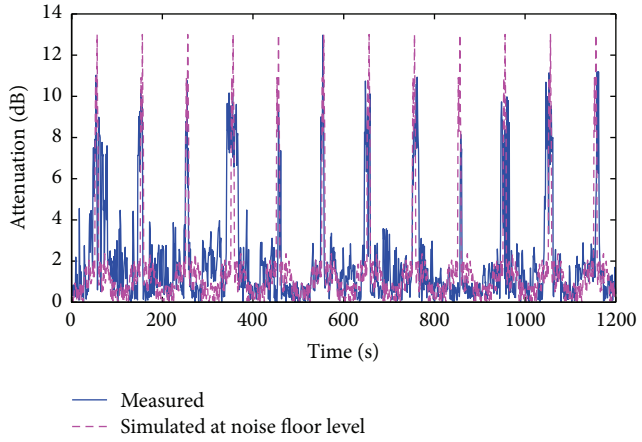

Figure 19: Measurement of attenuation inasmuch (PAs) + simulation at noise floor level, time series.

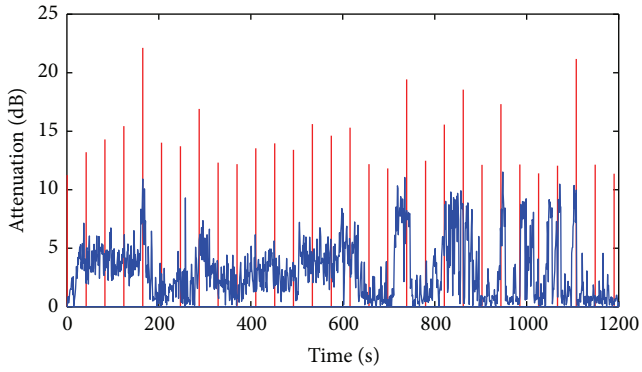

Figure 20: Total attenuation (PAs) + rain versus time series synthesizer.

Referring to Figure 20, the attenuation due to power arches supply and rain is cumulatively plotted. The magnitudes of attenuation reported from rain were less than power arches supply at all test times. The highest difference is set to zero at 22.12 dB at 170 seconds while the lowest difference is set to 11.25 dB at 1190 seconds. Otherwise, the difference value between rain attenuation and PAs was almost fluctuated at all readings.

5. Conclusion

The current study has quantified the reasons for the decrease in channel quality of mobile scenario at Ku-band, which is the most widely used channel frequency band for communication satellites in the tropics. Signal attenuation has been found to increase up to 12.5 dB on a speeding train due to PAs with heavy rainfall of 11.3 dB at high elevation angle (77.5°). This attenuation owing to PAs and rain resulted in serious problems to the communication link, especially in the open area. The change in train speed caused lower signal speed that exceeded 100 km/hr. It is also noted that the train speed causes at most around 1.2 dB of attenuation. Our study has developed a new measurement setup to predict the total attenuation of the power arches supply with the attenuations resulting from rain in tropical region with accuracy as high as possible. A system design based on one of the prediction models can estimate the exact attenuations resulting from PAs with rain for Malaysia as an example for tropical region and can produce a suitable design for better communication service in the future.

Conflict of Interests

The authors declare that there is no conflict of interests regarding the publication of this paper.

Acknowledgment

This project entitled S-PROMOTE: Propagation Measurement for Train Environment over GEO Satellite Network is funded by Malaysia Ministry of Education (MoE) under the Exploratory Research Grant Scheme (ERGS), Project code ERGS/1-2012/5527096.

References

[1] G. Maral and M. Bousquet, *Satellite Communications Systems: Systems, Techniques and Technology*, John Wiley & Sons, 2011.

[2] B. M. Owen, *The Internet Challenge to Television*, Harvard University Press, 2009.

[3] P. D. Karabinis, M. Kornby, and N. R. C. Rydbeck, "Dual-mode satellite/cellular phone architecture with physically separable mode," Google Patents, 2000.

[4] D. Marpaung, L. Zhuang, M. Burla et al., "Towards a broadband and squint-free Ku-band phased array antenna system for airborne satellite communications," in *Proceedings of the 5th European Conference on Antennas and Propagation (EUCAP '11)*, pp. 2623–2627, April 2011.

[5] A. Abele, F. Perez-Fontan, M. Bousquet et al., "A new physical-statistical model of the land mobile satellite propagation channel," in *Proceedings of the 4th European Conference on Antennas and Propagation (EuCAP '10)*, pp. 1–5, April 2010.

[6] A. Abdi, W. C. Lau, M.-S. Alouini, and M. Kaveh, "A new simple model for land mobile satellite channels: first- and second-order statistics," *IEEE Transactions on Wireless Communications*, vol. 2, no. 3, pp. 519–528, 2003.

[7] I. ITU, *681-7 Propagation Data Required for the Design of Earth-Space Land Mobile Telecommunication Systems*, ITU, 2009.

[8] P.-D. Arapoglou, K. P. Liolis, and A. D. Panagopoulos, "Railway satellite channel at Ku band and above: composite dynamic modeling for the design of fade mitigation techniques," *International Journal of Satellite Communications and Networking*, vol. 30, no. 1, pp. 1–17, 2012.

[9] S. Scalise, R. Mura, and V. Mignone, "Air interfaces for satellite based digital TV broadcasting in the railway environment," *IEEE Transactions on Broadcasting*, vol. 52, no. 2, pp. 158–166, 2006.

[10] A. D. Panagopoulos, P. M. Arapoglou, and P. G. Cottis, "Satellite communications at KU, KA, and V bands: propagation impairments and mitigation techniques," *IEEE Communications Surveys & Tutorials*, vol. 6, no. 3, pp. 2–14, 2004.

[11] J. S. Mandeep, Y. Y. Ng, H. Abdullah, and M. Abdullah, "The study of rain specific attenuation for the prediction of satellite

propagation in Malaysia," *Journal of Infrared, Millimeter, and Terahertz Waves*, vol. 31, no. 6, pp. 681–689, 2010.

[12] S. Cioni, C. P. Niebla, G. S. Granados, S. Scalise, A. Vanelli-Coralli, and M. A. V. Castro, "Advanced fade countermeasures for DVB-S2 systems in railway scenarios," *EURASIP Journal on Wireless Communications and Networking*, vol. 2007, Article ID 49718, 2007.

[13] ITU, "P.1853-0 Tropospheric attenuation time series synthesis," ITU, 2009.

[14] H. A. Mohammed, M. J. N. Sibley, and P. J. Mather, "Investigation of Doppler Effects on high mobility OFDM-MIMO systems with the support of High Altitude Platforms (HAPs)," *Journal of Physics: Conference Series*, vol. 364, no. 1, Article ID 012048, 2012.